Excitons in V-Shaped and T-Shaped Semiconductor Quantum Well Wires

Dirk Brinkmann, Axel Löffler, Guy Fishman

Excitons in V-Shaped and T-Shaped Semiconductor Quantum Well Wires

Dirk Brinkmann, Axel Löffler and Guy Fishman (*)

Laboratoire de Spectrométrie Physique (**), Université Joseph Fourier, Grenoble 1, BP 87, 38402 Saint Martin d'Hères Cedex, France

(Received 17 February 1997, revised 28 May 1997, accepted 23 June 1997)

PACS.73.20.Dx – Electron states in low-dimensional structures (superlattices, quantum well structures and multilayers)
PACS.78.55.Cr – III-V semiconductors

Abstract. — We give a general framework for describing electronic states in isolated quantum wires. It provides a description of both the conduction band and the valence band, taking full account of the complexity of the Γ_8 valence band. This is applied to T-shaped wires and V-shaped wires. To make a useful comparison with experimental results we calculate the exciton Rydberg. We show that in the case of the T-shaped wires hole confinement is due to the interaction with the confined electron and not due to the confining potential: the red shift of the wire exciton line with respect to that of the quantum well is mainly due to the decrease of the electron confinement energy and only partially to the increase of the exciton Rydberg. The experimental results are reproduced with no adjustable parameters.

1. Introduction

Among the quantum wells (QWs) liable to describe the potential in quantum physics, the finite square QW plays a special role because the Hamiltonian is exactly soluble. This means that the Schrödinger equation can be reduced to a transcendental equation which gives all the coefficients of the analytical shape of the wave function. Finite square QWs are not very common except in two-dimensional (2D) semiconductors where the electrons are confined in one direction, so that the finite square QW describes very well the physical situation in the effective mass approximation, which is the framework of this paper. In 2D semiconductors, two masses, one inside the well and one in the barrier, are necessary to describe the conduction electron but this again leads to a transcendental equation [1]. In a quantum wire, henceforth called a wire, the electrons are confined in a 2D potential and the problem is different; the potential is not separable, except in very special cases, and the Schrödinger equation is a partial differential equation: it is no longer a trivial problem to obtain the electron energy even for the conduction band. The problem is not academic because of progress in making semiconductors wires (also called one-dimensional semiconductors) which invites comparison between the experimental results, particularly the photoluminescence lines, and the theory [2–16]. In recent years, measurements have been performed on wires of several

(*) Author for correspondence (e-mail: guy.fishman@ujf-grenoble.fr)
(**) CNRS UMR 5588

types: V-shaped quantum wires (VWI) [5,6,9,10], T-shaped quantum wires (TWI) [3,7,16], and quantum wires with Strain-induced lateral confinement (SWI) [2,13]. A theoretical study of SWIs has already been published [13,14] so that in the present paper we deal only with VWIs and TWIs. Although the shapes are very different these wires have at least three points in common: i) the potential is not separable, ii) the wires are isolated and iii) the three types of wires are parallel to the [110] direction (or any equivalent crystallographic direction). From a theoretical viewpoint the main problem is linked to the fourfold degeneracy of the valence band [17]. The problem of the valence band dispersion was first solved by assuming either that the potential is separable [18], or that the wires form a superlattice [19], the wires being oriented along [001]. Recently the valence band dispersion was calculated in a VWI [4,8,15], the wire being oriented along [110], and in a TWI [11,15]. To perform this calculation we use the same symmetrized Luttinger Hamiltonian as in references [8,18] and we take into account the exact (finite) potential. However the luminescence lines were attributed to excitons in the wire so that it is not enough to know the conduction electron energy and the valence band dispersion: a meaningful comparison between the experimental and theoretical transition energies requires the knowledge of the exciton Rydberg as well. The aim of this paper is to present a calculation of the excitonic energies in VWIs and TWIs taking into account the exact valence band symmetry. This provides an unambiguous understanding of the origin of the luminescence lines reported in references [3,5].

Throughout the present paper, the direction along the length of the wire is taken as both the z-axis and the spin quantization axis, and the radial vector is $\rho = (x, y)$. The free electron mass is taken as unity.

2. V-Shaped Quantum Wires

We deal with the VWI whose shape is described in reference [5]. The GaAs wire is surrounded by a barrier in GaAlAs. The photoluminescence (PL) spectra give the energy of the e1-h1 and e2-h2 excitons with which we are dealing. We need to know the exact shape of the VWI to perform the calculation. We start from a TEM micrograph from reference [20] and model the shape of the boundary between GaAs and GaAlAs with an accuracy of the order of one monoatomic layer: to go beyond this accuracy has no physical meaning. Figure 1 gives the potential modelization we use.

We then calculate the energies and the wave functions following the multi-component variational method of reference [21], which is suited to isolated QWs and which we have extended for isolated wires along the [110] direction. We recover the (envelope) wave function $\chi_e = \chi_e(\rho_e)$ of the conduction band [5] and the wave function $\chi_h = \chi_h(\rho_h)$ of the valence band [10,15]. In a wire the $|JM\rangle$ components are strongly mixed even at $k = 0$, where k is the one-dimensional wave vector. The hole wave function χ_h has two components $\chi_h = f^{(h)}_{\pm 3/2}(\rho_h)\ |3/2 \pm 3/2\rangle + f^{(h)}_{\mp 1/2}(\rho_h)\ |3/2 \mp 1/2\rangle$ (the two functions are Kramers conjugate). The electron and hole ground state (e1-h1) wave functions are given in Figure 2 and the first excited state (e2-h2) wave functions are shown in Figure 3. Both are given for a zero wave vector. We have obtained the dispersion curve of the conduction band and the valence band as well. The first two conduction bands (e1 and e2) are described by an effective mass of 0.067: We have taken into account the larger mass in the barrier but this does not change the e1 and e2 masses up to 0.01 Å^{-1}. The first two valence bands (h1 and h2) are quite reasonably described by masses $m_{h1} = 0.13$ and $m_{h2} = 0.20$ respectively up to a wave vector equal to 0.01 Å^{-1}, as shown in Figure 4. Owing to the structure of χ_h the symbols h1 or h2 merely index the valence subbands without any relation to heavy or light holes with the quantization

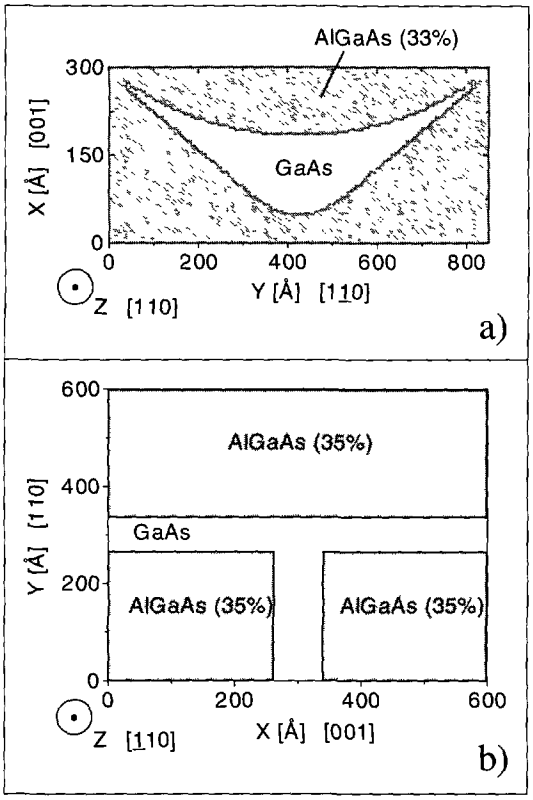

Fig. 1. — Potential profiles of a) the V-shaped wire (VWI) and b) the T-shaped wire (TWI) studied in this paper. The modelization of the VWI is based on reference [20]. The geometry of the TWI is that given in reference [3].

axis parallel to the wire. However if the quantization axis is perpendicular to the wire the holes are mainly heavy or light with the terms usual in quantum wells [15].

Once the masses and the envelope functions are known, we are in a position to calculate the exciton by a variational approach of the type often used in QWs [22]. The exciton Hamiltonian is $H = p^2/2\mu - e^2/\varepsilon r$ where ε is the background dielectric constant, $1/\mu = 1/m_e + 1/m_h$ where $m_h = m_{h1}$ for the e1-h1 exciton and $m_h = m_{h2}$ for the e2-h2 exciton. With this Hamiltonian, the potential confinement is taken into account *via* the trial function $\Psi = \chi_e \chi_h e^{-|z|/\lambda}$ where z is the in-wire distance between the electron and the hole and λ is a variational parameter that plays the role of a Bohr radius. The form of the hole wave function leads to a two component exciton wave function in a wire. We find that the Bohr radius λ is equal to 193 Å for e1-h1 and 203 Å for e2-h2: these values are consistent with the condition that λ^{-1} (about 0.005 $Å^{-1}$) is far smaller than the range of validity of the effective mass description of the carriers (0.01 $Å^{-1}$) as shown in Figure 4. Were this condition not fulfilled, the exciton calculation would have no meaning. The exciton Rydbergs are respectively 9.5 and 8.0 meV. This small difference is due to the fact that the Bohr radii are close because the reduced masses μ are not very different (respectively 0.044 and 0.050). Thus the difference between the exciton transition energies results mainly from different confinement energies for the excitons e1-h1 and e2-h2 (called $n_x = 1$ and $n_x = 2$ in Ref. [5]).

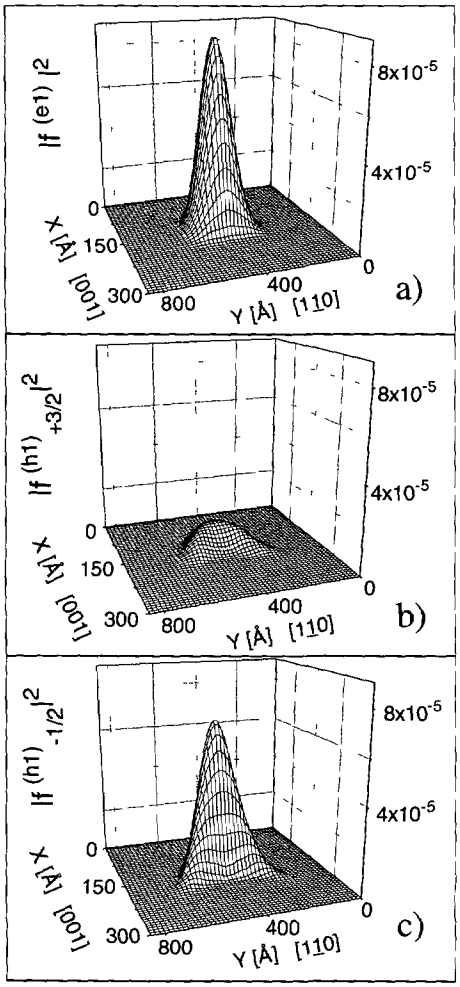

Fig. 2. — Probability of finding the electron and the hole in their ground state (e1-h1) in the V-shaped wire (VWI) described in reference [12]. The wave vector parallel to the wire is equal to zero. a) The squared modulus of the conduction band ground state wave function. b) The squared modulus of the $|3/2 \pm 3/2\rangle$ component of the valence band ground state wave function h1. c) The same as in b) but for the $|3/2 \mp 1/2\rangle$ component. The spin quantization axis is parallel to the wire throughout the present paper.

The exact shape of the VWI used in the experiments has a large influence of the energies of excitons e1-h1 and e2-h2 but a smaller influence on the splitting between these two lines. Thus, although we did not perform a calculation on exactly the same sample as in reference [5], it makes sense to compare the calculated splitting to the experimental one. The energy splitting calculated from the data of reference [20] between the excitons e1-h1 and e2-h2 is 22 meV while the experimental splitting in reference [5] is measured to be 20 meV with a FWHM of the order of 10 meV. This fully confirms the interpretation made by Rinaldi *et al.* of their two lines [5].

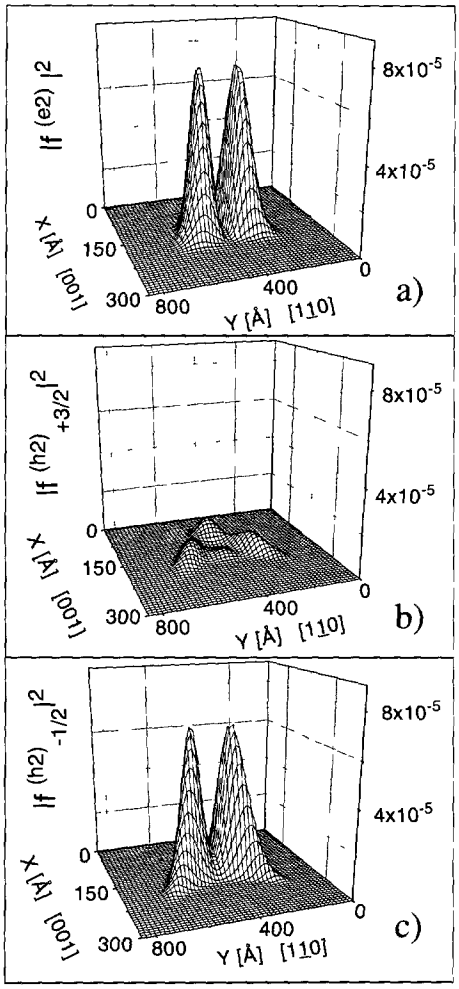

Fig. 3. — Probability of finding the electron and the hole in their first excited state (e2-h2) in the same VWI as in Figure 2. The wave vector parallel to the wire is equal to zero. a) The squared modulus of the first excited state wave function of the conduction band. b) The squared modulus of the $|3/2\ \pm 3/2\rangle$ component of the valence band first excited state wave function h2. c) The same as in b) but for the $|3/2\ \mp 1/2\rangle$ component.

3. T-Shaped Quantum Wires

The TWI fabricated with GaAs-GaAlAs is a different case. We are interested in the low excitation PL spectra in Figure 4 of reference [3], where the various lines are identified as originating from the TWI and from the two QWs that form the vertical part of the T (growth axis in the [001] direction) and the horizontal part of the T (growth axis in the [110] direction) so that the wire is along the [1 −1 0] direction. The geometry is given in Figure 1. In the following we write 001 and 110 as subscripts to distinguish the two QWs. The width of each QW is 70 Å; each [001] QW is separated by 380 Å.

First we calculate the energies of the QWs whose valence band dispersion curves are given in Figure 5. The calculation is performed in the axial approximation which gives averages over all the directions of the in-plane wave vector **k**. The confinement energies at $\mathbf{k} = \mathbf{0}$ are

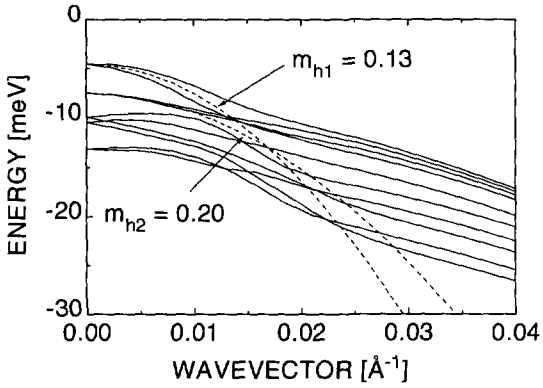

Fig. 4. — Dispersion curve of valence band energy of the VWI. The VWI has no inversion center, so the spin degeneracy is lifted. The wave vector is parallel to the wire. The indices h1 and h2 correspond to the hole ground state and to the first excited state but not to the heavy or light hole which has no meaning in such a wire (see Figs. 1 and 2). The average masses $m_{h1} = 0.13$ and $m_{h2} = 0.20$ are valid up to wave vectors about equal to 0.01 Å^{-1}, that is larger than the inverse of the Bohr radius of the exciton e1-h1 and e2-h2 (see text).

$E_e = 55.1$ meV for the electron in both the QWs (the conduction electron mass is isotropic) and $E_{h001} = 12.6$ meV and $E_{h110} = 7.6$ meV, while the masses m_h of the first valence band in each QW are $m_{h001} = 0.19$ and $m_{h110} = 0.17$: these masses are used to calculate the exciton Rydberg in the two QWs (see below). For the [001] QW the symbols hhn and lhn mean heavy and light hole as usual. For the [110] QW the symbols 'hhn' and 'lhn' mean heavy and light hole only in the axial approximation used here. In the general case the wave functions hhn and lhn do not correspond to the wave functions $|3/2 \pm 3/2\rangle$ and $|3/2 \pm 1/2\rangle$ respectively, even at $\mathbf{k} = \mathbf{0}$ (see Ref. [21]). The range where the effective mass of the hole has a meaning is of the order of 0.02 Å^{-1} The exciton Rydberg R_X calculated by a method similar to that used in Section 2 is 7.2 meV for the vertical QW and 7.0 meV for the horizontal QW. The Bohr radii are respectively 137 and 147 Å, whose inverse is smaller than 0.02 Å^{-1}: thus the calculation is consistent. The exciton transition energies are then $E_X = E_G + E_e + E_h - R_X = E_G + \Delta E_X$ so that E_X is 1579.9 meV for the vertical QW and 1575.1 meV for the horizontal QW (E_G is the GaAs bandgap). In reference [3] the PL energies of the two QWs are 1579 and 1583 meV with a FWHM of the order of 2 meV.

Now we come to the wire. First we suppose that the wires are isolated. The conduction band dispersion curve looks like that of the bulk: The 1D conduction mass is practically unchanged (0.068 instead of 0.067) [23]. On the contrary the valence band dispersion is quite different and is given in Figure 6. The hole effective mass, valid up to a wave vector larger than 0.01 Å^{-1}, is equal to 0.12. Once the energy is known we can get the wave functions, which are given for a zero wave vector in Figure 7. More precisely, Figure 7 gives the probability of finding the electron in a wire: for the electron it is valid to suppose the wire isolated [3]. The electron confinement energy is $E_e = 46.4$ meV. The same figure also gives the probability that a hole is present, which is the sum of the squares of the moduli of the two components. Clearly, as far as the hole is concerned the wire cannot be considered as isolated. The reason that the hole is poorly localized in the wire is the following: the confinement energy E_{h110} is 5 meV lower than the confinement energy E_{h001} (see Fig. 5) and therefore the hole is mainly confined in the 110 QW. Were the TWI built with axes rotated by 90 degrees (inversion of the [001] and [110] axes) the hole confinement would be different.

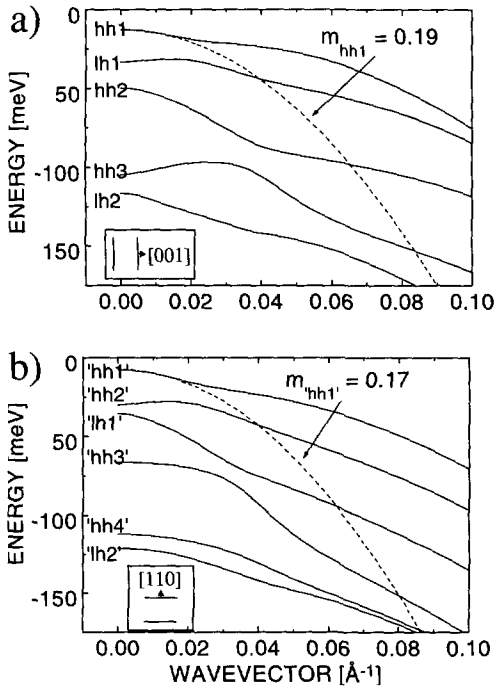

Fig. 5. — a) Valence band dispersion curve for the quantum well whose growth axis is in the [001] direction and which forms the vertical part of the T-shaped quantum wire (TWI) described in reference [3]. b) The same for the quantum well whose growth axis is in the [110] direction and which forms the horizontal part of the TWI. The masses $m_{h001} = 0.19$ and $m_{h110} = 0.17$ are used in the variational calculation of the two-dimensional exciton Rydberg. The indices hhn and lhn for the growth axis in the [001] direction correspond to the usual heavy and light holes in a two-dimensional semiconductor. The indices 'hhn' and 'lhn' for the growth axis in the [110] direction correspond mainly, but not exactly, to heavy and light holes in a two-dimensional semiconductor (see text).

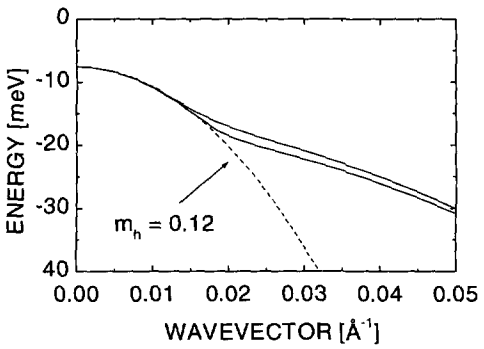

Fig. 6. — Valence band dispersion curve for the wire of the TWI structure. The calculation is made as if the wires were isolated. See text regarding the limit of validity of this description.

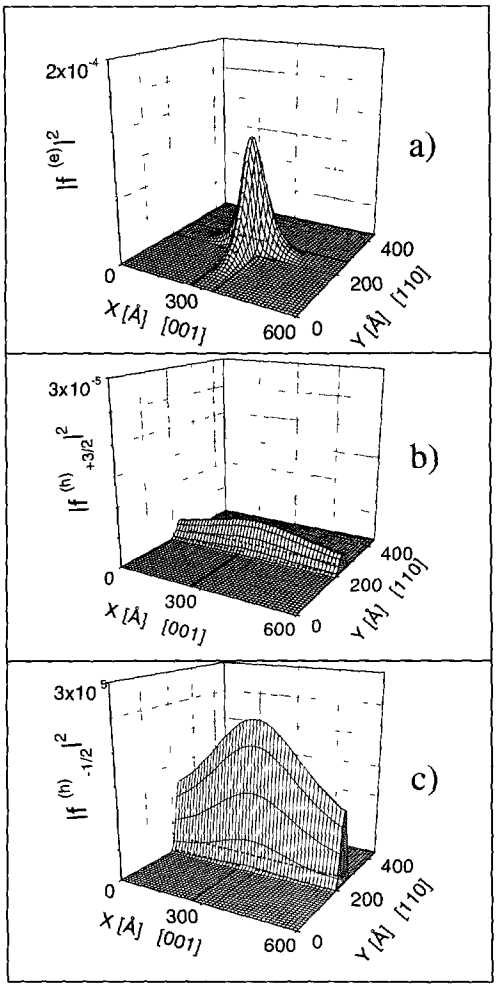

Fig. 7. — Probability of finding the electron and the hole in their ground state (e1-h1) in the T-shaped wire (TWI). The wave vector parallel to the wire is equal to zero. a) The squared modulus of the conduction band ground state wave function. b) The squared modulus of the $|3/2 \pm 3/2\rangle$ component of the valence band ground state wave function h1. c) The same as in b) but for the $|3/2 \mp 1/2\rangle$ component. The calculation was performed assuming the wires, separated by 380 Å, are isolated. The figure shows that this is true for the electron but not for the hole, which is not localized in a wire: the hole will be localized by the attraction of the confined electron as shown in Figure 8.

The hole being weakly localized, the validity of the assumption that the wires are isolated is questionable and one could think of calculating the dispersion curve for coupled wires. However we must keep in mind that the aim is to calculate the exciton Rydberg which means here an exciton where only the electron is well localized. The method of the preceding section is not usable and we are led to use another method to calculate the excitonic transition energy E_X, namely localization of the hole by the confined electron, used by Peter *et al.* in 2D semiconductors [24]. This is the reason why we have not calculated the hole dispersion curve for a coupled wire: in any case neither the latter curve nor the periodic wave function would be useful in the method of Peter *et al.* Now we have to extend it here to 1D semiconductors.

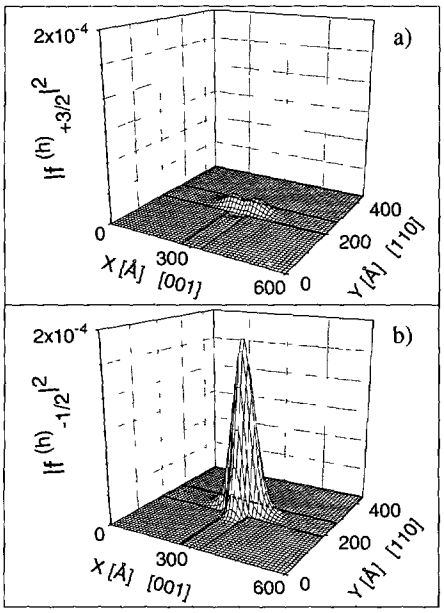

Fig. 8. — The figure gives the squared modulus of the two hole components of the exciton in the TWI, *i.e.* both the valence potential and the attraction of the hole by the confined electron are taken into account contrary to the case of Figure 5 where only the valence potential is taken into account. a) The squared modulus of the $|3/2\ \pm 3/2\rangle$ component of the hole wave function. b) the same as in a) but for the $|3/2\ \mp 1/2\rangle$ component.

This leads to a problem that is specific to quantum wires: the hole attracted by the electron is a two-dimensional hole; what hole mass should be used in such a calculation, and more precisely which is the 2D mass to be introduced? For the reason stated above we take the mass in the horizontal well, namely 0.17. The electron mass and the hole mass being defined, the calculation is more complicated than in 2D semiconductors because we have to calculate a two-component hole function. Formally the result has the same shape as that given in the VWI section, but *here the components are obtained from a calculation of the hole attracted by the electron and not from a calculation of the hole localized directly by the wire.*

The two components are given in Figure 8 which shows unambiguously that the hole is now localized on a wire. The energy of this hole, localized both by the wire potential and by the Coulomb interaction with the electron, is $E_{\mathrm{hC}} = -4.4$ meV. The excitonic transition energy $E_{\mathrm{X1D}} = E_{\mathrm{G}} + E_{\mathrm{e}} + E_{\mathrm{hC}} = E_{\mathrm{G}} + \Delta E_{\mathrm{X}}$ is then 1561.4 meV. The experimental result is approximatively 1564 meV (the line width is of the order of 7 meV). This corresponds to the experimentally observed shift, 17 meV, noted in reference [3] between the average of the QWs lines (1581 meV) and the wire exciton. We can now look at how we obtain this difference in our calculation. The result is summarized in Figure 9 where the results for the QWs are the average of the energies of the two QWs. We see that the difference between the average exciton energy 1577.5 meV of the two QWs and $E_{\mathrm{X1D}} = 1561.4$ meV is 16.1 meV, which is to be compared to the value 17 meV quoted in reference [3]. Although we do not have exactly the same interpretation as that of reference [3], we point out here that we end up with the same result as the experiment, so that there is no doubt as to the origin of the lines.

Before concluding we note that we use the same kind of calculations that are known to work in two-dimensional semiconductors. It is therefore not very surprising that they work

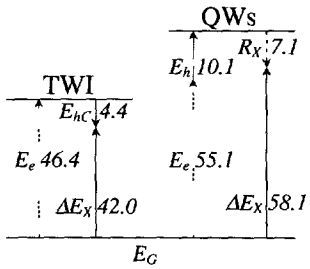

Fig. 9. — This diagram shows the different energies that play a role in the TWI. The energy gap E_G is taken as the origin of energy. In the left column the energies are those of the wire; E_e is the confinement energy of the electron; the hole energy $E_h = E_{hC}$ is negative because the hole is confined by the Coulomb interaction of the electron. In the right column the mean energies of the two quantum wells are given in order to allow comparison with the results of reference [3]; E_e (E_h) is the electron (hole) confinement energy. R_X is the Rydberg energy of the exciton. In both cases $E_X = E_G + \Delta E_X$ is the theoretical luminescence exciton energy. The theoretical difference $58.1 - 42 = 16.1$ meV is to be compared with the experimental result: 17 meV in reference [3].

in one-dimensional semiconductors as well. Using the same method for the dispersion curve calculation as that used for two-dimensional semiconductors [21] we are led to diagonalize a Hermitian matrix of dimensions 30×4 dimension for the valence band in a QW (30: basis dimension, 4: valence band degeneracy) and $30 \times 30 \times 4$ in a wire: the computation time is tremendously increased in the latter case.

4. Conclusion

In conclusion, a theoretical study of excitons in quantum wires provides an unambiguous identification of the photoluminescence lines observed. The full calculation shows that in all of the wires only the electron is confined, in contrast to the hole which is well confined in the VWI and poorly confined in the TWI. In the latter case the exciton is linked to the wire only because the hole is confined by the Coulomb attraction of the electron. Finally the red shift of the wire's photoluminescence with respect to the QW photoluminescence is due mainly to the decrease of the electron confinement energy. In other words the one-dimensional exciton Rydberg is not always increased with respect to the two-dimensional exciton Rydberg. If the surrounding potential were infinite this would always be the case, but in a real wire the extent of the wire wave functions can be larger than the quantum well wave functions so that a numerical calculation is needed to make an accurate comparison.

Acknowledgments

We acknowledge useful discussions with R. André, C. Gourgon, Le Si Dang, H. Mariette and P. Valiron and thank E. Geissler and R. Cox for a critical reading of the manuscript. We thank the Observatoire de Grenoble and the "Centre Grenoblois de Calcul Vectoriel" for providing us with computer facilities.

References

[1] See for example Altarelli M., Semiconductor Superlattices and Heterojunctions, G. Allan, G. Bastard, N. Boccara, M. Lannoo and M. Voos, Eds. (Springer Verlag, Berlin, 1986) p. 12.

[2] Gershoni D., Wiener J.S., Chu S.N.G., Baraff G.A., Vandenberg J.M., Pfeiffer L.N., West K., Logan R.A. and Tanbuk-Ek T., *Phys. Rev. Lett.* **65** (1990) 4011.
[3] Wegscheider W., Pfeiffer L.N., Dignam M.M., Pinczuk A., West K.W., McCall S.L. and Hull R., *Phys. Rev. Lett.* **71** (1993) 4071.
[4] Citrin D.S. and Yia-Chung Chang, *IEEE J.Quantum Electron.* **29** (1993) 97.
[5] Rinaldi R., Cingolani R., Lepore M., Ferrara M., Catalano I.M., Rossi F., Rota L., Molinari E., Lugli P., Marti U., Martin D., Morier-Gemoud F., Ruterana P. and Reinhart F.K., *Phys. Rev. Lett.* **73** (1994) 2899.
[6] Rinaldi R., Ferrara M., Cingolani R., Marti U., Martin D., Morier-Gemoud F., Ruterana P. and Reinhart F.K., *Phys. Rev. B* **50** (1994) 11795.
[7] Someya T., Akiyama H. and Sakaki H., *Phys. Rev. Lett.* **74** (1995) 3664.
[8] Yi J.C. and Dagli N., *IEEE J.Quantum Electron.* **31** (1995) 208.
[9] Kapon E., Biasol G., Hwang D.M., Walther M. and Colas E., *Solid State Electron.* **40** (1996) 815.
[10] Goldoni G., Rossi F., Molinari E., Fasolino A., Rinaldi R. and Cingolani R., *Appl. Phys. Lett.* **69** (1996) 2965.
[11] Gislasson H., Langbein W. and Hvam J.M., *Appl. Phys. Lett.* **69** (1996) 2948.
[12] Langbein W., Lüerβen D., Kalt H., Braun W. and Ploog K., *Phys. Rev. B* **53** (1996) 15473.
[13] Mariette H., Brinkmann D., Fishman G., Góurgon C., Le Si Dang and Löffler A., *J. Cryst. Growth* **159** (1996) 418.
[14] Brinkmann D., Fishman G., Gourgon C., Le Si Dang, Löffler A. and Mariette H., *Phys. Rev. B* **54** (1996) 1872.
[15] Goldoni G., Rossi F., Molinari E. and Fasolino A., *Phys. Rev. B* **55** (1997) 7110.
[16] Vouilloz, Oberli D.Y., Dupertuis M.-A., Gustafsson A., Reinhardt F. and Kapon E., *Phys. Rev. Lett.* **78** (1997) 1580.
[17] Luttinger J.M., *Phys. Rev.* **102** (1956) 1030.
[18] Bockelmann U. and Bastard G., *Phys. Rev. B* **45** (1992) 1688; Schult R.L., Ravenhall D.G. and Wyld H.W., *Phys. Rev. B* **39** (1989) 5476.
[19] Baraff G.A. and Gershoni D., *Phys. Rev. B* **43** (1991) 4011.
[20] Jouneau P.H., Bobard F., Marti U., Robadey J., Filipowitz F., Martin D., Morier-Gemoud F., Silva P.C., Magnenat Y. and Reinhart F.K., Proceedings of Microsc. Semicond. Mater. Conf., Oxford, *Inst. Phys. Conf. Ser.* **146** (1995) 371; Jouneau P.H., private communication.
[21] Fishman G., *Phys. Rev. B* **52** (1995) 11132.
[22] Bastard G., Wave Mechanics Applied to Semiconductor Structures (Les Éditions de Physique, Les Ulis, 1988).
[23] The slight difference between the values 0.068 and 0.067 results from the fact we take into account the larger effective mass inside a GaAlAs barrier. We do not take into account the non-parabolicity of the conduction mass. In the same way we take into account the different values of the Luttinger parameters in the well and in the barrier, but inside each material the bands are supposed to be parabolic, or in other words, the Luttinger parameters are constant inside each barrier.
[24] Peter G., Deleporte E., Bastard G., Berroir J.M., Delalande C., Gil B., Hong J.M. and Chang L.L., *J. Lumin.* **52** (1992) 147; Barrau J., Amand T., Brousseau M., Simes R.J. and Goldstein L., *J. Appl. Phys.* **71** (1992) 5768.